



## Molecular dynamics of 5-HT<sub>1A</sub> and 5-HT<sub>2A</sub> serotonin receptors with methylated buspirone analogues

Agnieszka Bronowska<sup>a,\*</sup>, Zdzisław Chilmonczyk<sup>b</sup>, Andrzej Leś<sup>a,c</sup>, Øyvind Edvardsen<sup>d</sup>, Roy Østensen<sup>e</sup> & Ingebrigt Sylte<sup>f</sup>

<sup>a</sup>Department of Chemistry, University of Warsaw, 1 Pasteura Str., 02-093 Warsaw, Poland; <sup>b</sup>Drug Institute, 30/34 Chełmska Str., 00-725 Warsaw, Poland; <sup>c</sup>Pharmaceutical Research Institute, 8 Rydygiera Str., 01-793 Warsaw, Poland; <sup>d</sup>Department of Pharmacology, Institute of Pharmacy, University of Tromsø, N-9037 Tromsø, Norway; <sup>e</sup>Department of Physics, University of Tromsø, N-9037 Tromsø, Norway; <sup>f</sup>Department of Pharmacology, Institute of Medical Biology, University of Tromsø, N-9035 Tromsø, Norway

Received 5 October 2000; accepted 12 November 2001

**Key words:** antidepressants, anxiolytics, buspirone analogues, ligand-receptor interactions, molecular dynamic, serotonin, serotonin receptors

### Summary

In the present study experimentally determined ligand selectivity of three methylated buspirone analogues (denoted as MM2, MM5 and P55) towards 5-HT<sub>1A</sub> and 5-HT<sub>2A</sub> serotonin receptors was theoretically investigated on a molecular level. The relationships between the ligand structure and 5-HT<sub>1A</sub> and 5-HT<sub>2A</sub> receptor affinities were studied and the results were found to be in agreement with the available site-directed mutagenesis and binding affinity data. Molecular dynamics (MD) simulations of ligand-receptor complexes were performed for each investigated analogue, docked twice into the central cavity of 5-HT<sub>1A</sub>/5-HT<sub>2A</sub>, each time in a different orientation. Present results were compared with our previous theoretical results, obtained for buspirone and its non-methylated analogues. It was found that due to the presence of the methyl group in the piperazine ring the ligand position alters and the structure of the ligand-receptor complex is modified. Further, the positions of derivatives with pyrimidinyl aromatic moiety and quinolinyl moiety are significantly different at the 5-HT<sub>2A</sub> receptor. Thus, methylation of such derivatives alters the 3D structures of ligand-receptor complexes in different ways. The ligand-induced changes of the receptor structures were also analysed. The obtained results suggest, that helical domains of both receptors have different dynamical behaviour. Moreover, both location and topography of putative binding sites for buspirone analogues are different at 5-HT<sub>1A</sub> and 5-HT<sub>2A</sub> receptors.

### Introduction

Serotonin receptors play a crucial role in many important processes in the central nervous system (CNS), including the regulation of mood, emotions, sleep and arousal mechanisms [1–6]. For this reason agents that interact with serotonin receptors are useful in the treatment of many psychiatric disorders, including anxiety and depression [1, 3, 6] and new drugs from this group are still desired. In order to design more potent

and effective serotonergic agents more knowledge about the molecular mechanism of ligand-receptor interactions is required.

To design ligands with selectivity towards different receptor subtypes is a big challenge for pharmacologists and medicinal chemists. This is complicated by the continuous identification of new receptor subtypes of the same family and also of new receptor families. The family of serotonin receptors is representative example in this context [7]. This family is divided into smaller groups and subfamilies, according to their ligand binding profile, interactions with

\* To whom the correspondence should be sent. E-mail: bronka@tiger.chem.uw.edu.pl

G protein and amino acid sequence. This classification brought more information about the mechanism of action of very potent anxiolytic, antidepressive and antipsychotic agents which interact with 5-HT<sub>1A</sub>, 5-HT<sub>1B</sub>, 5-HT<sub>2A/2C</sub> and 5-HT<sub>2B</sub> serotonin receptor subtypes [8, 9]. Some of these compounds are very effective in the treatment of panic and general anxiety disorder, obsessive-compulsive disorder, and many more [10].

In the present study we have investigated by computational methods the interactions of 5-HT<sub>1A</sub> and 5-HT<sub>2A</sub> receptor models with a series of buspirone analogues possessing a methyl group at the piperazine ring (Table 1). Buspirone is a well-known partial agonist of 5-HT<sub>1A</sub> serotonin receptors [7], frequently used in the therapy of various forms of anxiety [10–15]. Buspirone is also used nowadays in depression [15–17], addictions [18–22] and autism treatment [23, 24]. The discovery of buspirone as a potent anxiolytic drug resulted in the synthesis and testing of several buspirone analogues as potential anxiolytic and antidepressive drugs [25, 26]. Pharmacological tests have shown that the anxiolytic effect of buspirone and its analogues is related to its 5-HT<sub>1A</sub> receptor affinity [7, 10, 12, 27]. The buspirone analogues have in general a number of important advantages over anxiolytics structurally related to benzodiazepines. These include: low toxicity, the lack of an associated sedative effect, and also the lack of addiction or withdrawal syndrome [27, 28]. Moreover, it was indicated that the mixed 5-HT<sub>1A/2A</sub> ligands could be very potent in treatment of various forms of anxiety and disorders that involve both anxiety and depression [29]. Detailed knowledge about the structure-activity relationships and receptor selectivity towards buspirone analogues seems to be important for understanding, on the molecular level, the mechanism of action of these anxiolytic drugs. This knowledge can be very helpful for medicinal chemists in rational design of new drugs with anxiolytic and antidepressive properties.

## Methods

### *Modelling of the ligands*

The starting geometries of all examined buspirone analogues (structures shown in Table 1) were taken from the crystal structures of buspirone and 4,4-dimethyl-1-[4-[4-(2-quinolinyl)-1-piperazinyl]butyl]-2,6-piperidinedione [31] and adapted for molecular

modelling with the Amber5.0 [34] program and MidasPlus [32] graphical software. The phthalimide fragment was created with the XLeaP [33] program, included in Amber 5.0. All investigated ligands had the nitrogen atom attached to the n-butyl moiety protonated (Table 1).

For each compound, after an initial geometry optimisation, restrained electrostatic potential fitted charges (RESPs) [35] were calculated using an *ab initio* RHF/6-31G\* basis set, by Gaussian94 [36]. Afterwards, the RESP charges were used in an energy minimisation, until convergence at the 0.002 kcal/mol · Å energy gradient differences between successive steps. Thereafter, a new set of RESP charges were calculated and used in subsequent energy minimisations.

For each ligand a set of conformers was generated by 750 ps Molecular Dynamics (MD) simulation, using the all-atom Amber5.0 force field. The MD simulations were performed at 310 K with velocity scaling, after an initial equilibrium period starting at 0.1 K. The step-length was 0.001 ps. The atomic coordinates were stored at 1 ps intervals.

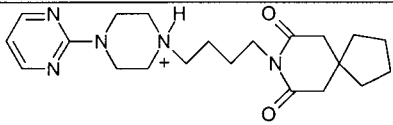
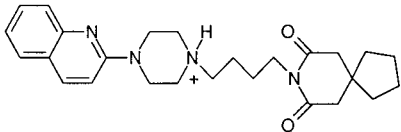
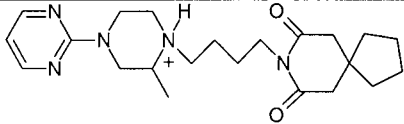
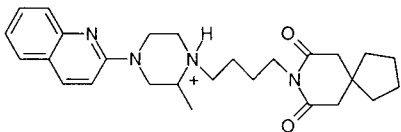
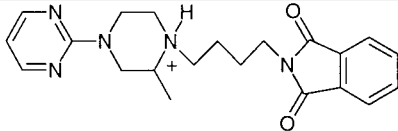
Potentially bioactive conformers were selected, using the method described in detail in our previous paper [30]. Conformations that fitted the biophore models for 5-HT<sub>1A</sub> and 5-HT<sub>2A</sub> (Figure 1) [30, 37] were selected: each conformer with a deviation within 1.15 Å in atomic distance between the selected atoms corresponding to the biophore model was energy minimised and the lowest-energy conformers were selected afterwards.

Solvent effects were included by using a distance-dependent dielectric function ( $\epsilon = 4r$ , where  $r$  is the inter-atomic distance in Å), without explicit solvent molecules, in all energy-refinements and MD simulations.

### *5-HT<sub>1A</sub> and 5-HT<sub>2A</sub> receptor modelling*

The 5-HT<sub>1A</sub> receptor model was constructed from the human 5-HT<sub>1A</sub> amino acid sequence [38]. Transmembrane helical domains (TMHs) were organised according to the suggested arrangement of the TMHs in G protein-coupled receptors (GPCRs) [39]. The helices were arranged such that amino acids in the sequence of the receptor at positions demonstrated to be important for ligand binding in other G protein-coupled receptors [40, 41] were facing the interior of the helical bundle. An initial model of the helical bundle was constructed from the previous 5-HT<sub>1A</sub> receptor model [42], with minor changes in tilting and

Table 1. Structures and affinity data of buspirone and its analogues. The affinities ( $K_i$ ) towards 5-HT<sub>1A</sub> and 5-HT<sub>2A</sub> receptors are given in nM

COMPOUND	STRUCTURE	$K_i$ (5-HT <sub>1A</sub> )	$K_i$ (5-HT <sub>2A</sub> )
BUSPIRONE		14 <sup>(75)</sup>	794 <sup>(72)</sup>
KASPAR		39 <sup>(31)</sup>	3442 <sup>(76)</sup>
MM2 (1)		167 <sup>(68)</sup>	1240 <sup>(68)</sup>
MM5 (2)		24 <sup>(68)</sup>	32 <sup>(68)</sup>
P55 (3)		126 <sup>(73)</sup>	9400 <sup>(73)</sup>

the axial rotations of some TMHs, further described elsewhere [30].

The N-terminus was copied from the previous 5-HT<sub>1A</sub> receptor model [42], energy-minimised and then connected to the TMH1. Initial structures of the extracellular loops (ECL)1–3, intracellular loops (ICL) 1 and 2, and the C-terminus were constructed by searching for loop segments in the Brookhaven PDB-database. The criteria used for the selection of these fragments were: the maximal sequence similarity and the lowest energy. The PDB identification codes for the sequence fragments used as initial structure of extramembranous domains of the 5-HT<sub>1A</sub> receptor model were: ICL1: 153L, ECL1: 2EQL, ICL2: 8CAT, ECL2: 3CYR, ECL3: 2REL, C-terminus: 2BUS. The initial structures of the receptor segments were constructed by changing the side chains of the found

loops into the side chains of the corresponding 5-HT<sub>1A</sub> receptor segments.

The structure of the third intracellular loop (ICL3) was generated by using the Predict-Protein server ([http://www.embl.columbia.edu/pp/submit\\_adv.html](http://www.embl.columbia.edu/pp/submit_adv.html)). The reason was that this loop of 5-HT<sub>1A</sub> consists of 133 amino acids, far too much to use sequence homology technique. A helical conformation was predicted for residues 4–11 and 93–111, while  $\beta$ -sheet conformation was predicted for residues 37–44 and 61–73. For the remaining part of the sequence, which was predicted in a random conformation, the same strategy as for the other extramembranous domains was applied, with the same criteria used. The PDB identification codes for the chosen segments are: 2BPA, 1BLA and 1NPO. Further details are described elsewhere [30].

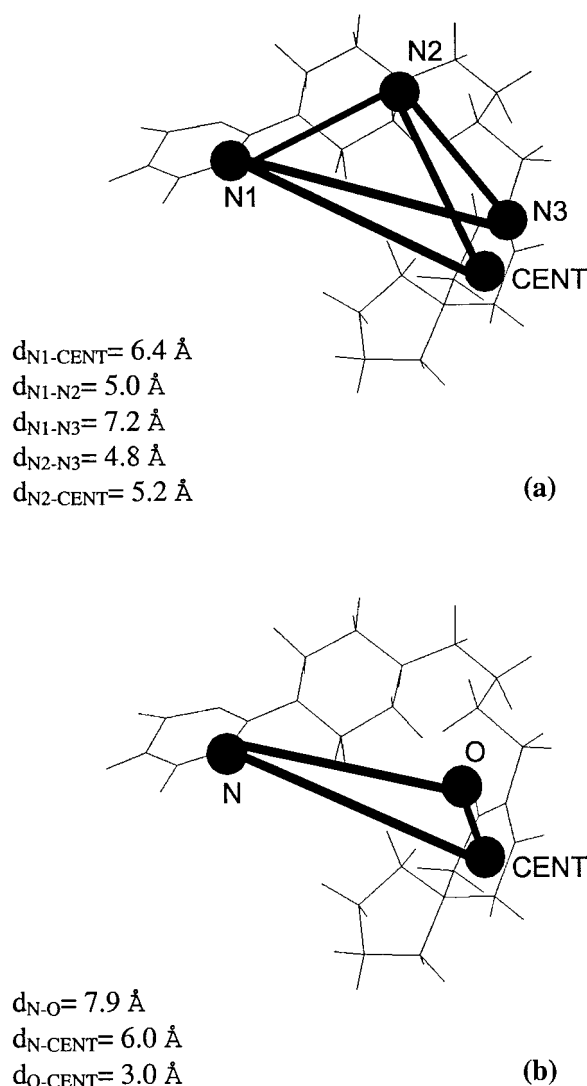


Figure 1. Biophore models for 5-HT<sub>1A</sub> (a) and 5-HT<sub>2A</sub> (b) receptors.

The receptor model was energy-refined in several steps: (a) 25 ps MD simulation at 300 K of the loops and terminals, while keeping the TMHs at a fixed position, (b) 25 ps of MD simulation (at 300 K) of all the side chains of the receptor model, (c) the entire receptor model was energy-minimised. A disulfide bridge between conserved cysteines C3.25(C109) and C187 in ECL2, known to form an important structural constraint in many GPCRs [43], was present during all simulations.

The model of the human 5-HT<sub>2A</sub> receptor was constructed from the amino acid sequence [43], by homology with the 5-HT<sub>1A</sub>. The TMHs and loops (ex-

cept for ICL3 and ECL2) of a 5-HT<sub>1A</sub> model were used as templates for 5-HT<sub>2A</sub> model construction. Models of the N- and C-terminal domains, ICL3 and ECL2 were constructed by searching for homologous fragments in the Brookhaven PDB database, with the same criteria as described for the 5-HT<sub>1A</sub> receptor model, and connected to the TMH bundle. The codes of the segments used for 5-HT<sub>2A</sub> loops construction: N-terminus: 1DIL, ECL1: 1SMD, ICL3: 1BUR, C-terminus: 2TMD.

Both energy-refined receptor models were used as starting structures for 30 ps of MD simulation. During these simulations the temperature was gradually increased from 0 to 300 K (50 K per each 5 ps of simulation). The obtained atomic coordinates were used for further 140 ps of MD simulation, at 300 K. The cut-off radius for non-bonded interactions during energy refinements and MD simulations of the receptor models was 12 Å. For both models the 30 atomic coordinate sets between 140 and 170 ps were used to calculate an average structure, which finally was energy-minimised until convergence at 0.002 kcal/mol Å.

To preserve the helical conformations of the TMHs, constraint forces corresponding to 5 kcal/mol Å<sup>2</sup> were applied between the backbone oxygen atom of residue  $n$  and the backbone nitrogen atom of residues  $n + 4$ , excluding prolines. Initial simulations indicated that such interhelical constraint forces were important to produce rigid body helical movements as observed in experimental studies [45, 46]. A similar strategy to constraining helices, together with distance-dependent dielectric function and dielectric constant  $\epsilon = 4r$ , has also been used previously during MD simulations of G protein-coupled receptors [47, 48].

#### Ligand-receptor interactions

The results from site-directed mutagenesis experiments [38, 49, 50] were used as guidelines in the docking of the ligands into the central cavity of the 5-HT<sub>1A</sub> receptor. After performing a preliminary study of several different positions, the two positions of each ligand giving the best ligand-receptor fits were selected for the further MM/MD calculations. The ligand-5-HT<sub>2A</sub> receptor complexes were constructed by analogy to the ligand complexes with the 5-HT<sub>1A</sub> receptor. The ligand-receptor complexes were energy-minimised and used as initial structures for 30 ps molecular dynamics simulation, performed as for the free receptors. The atomic coordinate sets obtained

after 30 ps of MD simulation were used as initial coordinates for further 140 ps MD simulation at 300 K, using constraints to preserve the helical conformation, as described for the free receptor. The 30 atomic coordinate sets obtained between 140 and 170 ps were used to calculate the average structures of ligand-receptor complexes, which finally were energy-minimised until convergence at a 0.002 kcal/mol Å energy gradient difference between successive steps.

## Results and discussion

Both receptor models examined in the present study were constructed with helical parts based on the projection map of visual rhodopsin [39]. This was a reasonable choice, since these receptors and rhodopsin belong to the same family of G protein-coupled receptors (GPCRs), which shares an overall structural similarity in the organisation of trans-membrane helices. However, during the preparation of this article the crystal structure of visual rhodopsin was published [51]. The rhodopsin x-ray structure showed that the overall helical packing and the orientation of the helices relative to each other were in very good accordance with the ligand-unbound 5-HT<sub>1A</sub> and 5-HT<sub>2A</sub> receptor models (Figure 2). In both our serotonin receptor models, the orientations of particular amino acid residues that are highly conserved among all the family A of GPCRs, were found at positions similar to those of the rhodopsin structure. Conserved asparagines in TMH1 and TMH7 (1.50 and 7.49) were found in similar conformation and orientation towards the interior helical bundle in rhodopsin (N55 and N382) and ligand-unbound serotonin receptors (N54 and N396 in 5-HT<sub>1A</sub>, N92 and N375 in 5-HT<sub>2A</sub>, respectively). Several residues in TMH6 which aromatic character, that are conserved among all family A members, were facing the inner receptor cavity in rhodopsin (F261, W265, and Y268), and the ligand-unbound 5-HT<sub>1A</sub> receptor (F364, W358, and F361). In the ligand-unbound 5-HT<sub>2A</sub> serotonin receptor (F331, W335, and F338) these residues were found slightly displaced from the inner cavity towards TMH7, however, this difference in TMH6 packing is not very dramatic. The orientation of conserved aspartic acid residue in TMH2 (D2.50) was very similar in rhodopsin and both ligand-unbound serotonin receptors. Also the orientations of conserved residues in TMH3 (3.45) and TMH7 (S7.46 and P7.50) were the same in all compared structures. Taken together, the

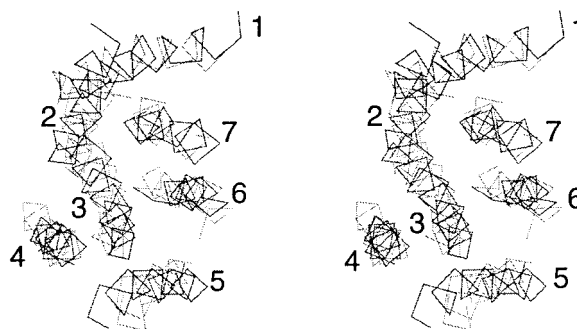


Figure 2. Superimposed seven transmembrane helical (TMH) bundle of 5-HT<sub>1A</sub> receptor model (dark grey) and rhodopsin crystal structure, viewed from the extracellular side.

comparison between our obtained models of ligand-unbound serotonin receptors and the crystallographic structure of rhodopsin proves the usefulness and validity of the present receptor models, although the helical bundles of these receptors were constructed using the projection map of rhodopsin as a guide and not its crystal structure. However, the conformation of both ligand-bound receptors differed from the crystal structure of rhodopsin. The helical rigid body movements, together with rotational changes and different tilting of the particular helices contributed mainly to these alterations. For instance, upon binding of compound (2), rigid body movements relatively to each other and also to remaining part of the helical bundle were observed for TMH3 and 6. During these displacements some differences in tilting were observed for TMH6, while tilting of TMH3 became practically unchanged. While interacting with (2), TMHs 4 and 5 changed its rotational orientation, and tilting of TMHs 2, 5 and 7 was found to be slightly altered. Also, orientations of many highly conserved amino acid residues changed upon the ligand binding (see 'Ligand-receptor interactions'). It is known that crystal structure of rhodopsin correspond to rhodopsin in its inactive state [51]. Therefore, observed differences between ligand-bound receptor form and x-ray structure of rhodopsin seem to reflect the ligand-mediated activation of the receptor.

The overall structures of the ligand-unbound 5-HT<sub>1A</sub> and the 5-HT<sub>2A</sub> receptor models are shown in Figure 3. The main differences between both receptor models were found in the structure of loops and termini (Figure 3) and in the interhelical hydrogen-bonding network (Table 2). These structural differences may contribute to the affinity differences for buspirone. The differences in the structure of loops

Table 2. Interhelical hydrogen bonds present in the structures of free 5-HT<sub>1A</sub> and 5-HT<sub>2A</sub> receptors. The one letter amino acid code, with the sequence number, are used for the amino acid residue specification, together with standard GPCRDB notation (in brackets)

5-HT <sub>1A</sub>	5-HT <sub>2A</sub>
N54(1.50)–D82(2.50)	N92(1.50)–D120(2.50)
T81(2.49)–N396(7.49)	D120(2.50)–S371(7.45)
D82(2.50)–P397(7.50)	D120(2.50)–S372(7.46)
D116(3.32)–N386(7.39)	D120(2.50)–N375(7.49)
S123(3.39)–S393(7.46)	S162(3.39)–S371(7.45)
S123(3.39)–N396(7.49)	

and terminal parts can influence the process of ligand recognition, binding and G protein interactions. The different architecture of the interhelical hydrogen-bonding network between the receptors may alter the helical packing and contribute to geometry differences at the receptor binding sites. The hydrogen bond between D116(3.32) and N386(7.40) in the free 5-HT<sub>1A</sub> receptor makes the region of the highly conserved aspartic acid in TMH3 narrower than in the free 5-HT<sub>2A</sub> receptor. Most of the amino acids involved in the hydrogen-bonding pattern of both receptors (except for N386(7.40) in 5-HT<sub>1A</sub> and S371(7.45) in 5-HT<sub>2A</sub>) are highly conserved in family A of the G protein-coupled receptors (GPCRs). It has been reported that the changes in the receptor hydrogen bonding network are important for several receptor's activation and signal transduction [30, 52, 53].

The main purpose of the MD simulations of the free receptor models was to obtain energetically stable receptor structures. These could be used afterwards for structural comparison with the ligand-receptor complexes after MD in order to investigate the ligand-induced structural changes of the receptor structure upon ligand binding. It has been proposed in a classical model of GPCR activation [54–56] that G protein-coupled receptors exist in equilibrium between two allosteric states, which are interconvertible. In the inactive state, predominating in the absence of agonist, structural constraints prevent the G protein coupling. In the active state of the receptor these structural constraints are relaxed and G protein can be coupled. The equilibrium between active and non-active states can be altered by ligand binding or mutation of the receptor [57–59]. According to the classical model, various levels of receptor activation are caused by these equilibrium alterations. The energy-minimised,

average receptor structure obtained after MD simulation brings information about the receptor state most frequently observed during the simulation. Therefore, comparison between average structures of the ligand-receptor complex and the free receptor may provide an information about structural changes upon ligand binding, that according to the classical model, should be correlated with the receptor activation.

### Ligand-receptor interactions

Available site-directed mutagenesis data, which were obtained for serotonin receptors and other GPCRs were used as a guide for ligand docking. These results allowed us to reduce significantly the number of ligand positions relative to the receptor models during the docking procedure, which might be interpreted as potential ligand-receptor interacting sites. These data together with binding affinity studies allowed for a more rationalised docking procedure that should lead to find the most realistic binding site. However, the binding modes in the present study should be further tested by site-directed mutagenesis studies, which may verify the validity of the present models.

Site-directed mutagenesis data obtained on the 5-HT<sub>1A</sub> and 5-HT<sub>2A</sub> receptors indicate the conserved aspartic acid residue (3.32) (D116 in 5-HT<sub>1A</sub> and D155 in 5-HT<sub>2A</sub>, respectively) as crucial for ligand binding [49, 60]. It has been suggested that this residue should interact directly with the protonated amino group of the ligand. It has also been demonstrated for visual rhodopsin that glutamic acid (3.32) corresponding to the aspartic acid in 5-HT<sub>1A/2A</sub> receptor, interact directly with retinal that is necessary for rhodopsin activation [61, 62]. It has also been reported that a highly conserved serine residue (S7.46) plays an important role in ligand-induced 5-HT<sub>1A</sub> receptor activation [38]. Site-directed mutagenesis experiments performed on the rat 5-HT<sub>2A</sub> receptor has suggested the important role of conserved aromatic residues in TMH6 in ligand-mediated receptor activation [63]. These residues should also participate in discrimination between ergoline and ergopeptine binding, by interacting with different ligand moieties in different manners [64]. Also, site-directed mutagenesis data obtained on the 5-HT<sub>1A</sub> receptor has shown the important role of the conserved N7.49 residue in receptor activation [38]. For each receptor, several ligand positions involving close contacts between different ligand moieties and residues indicated by mutagenesis experiments as important for ligand binding (i.e., aromatic

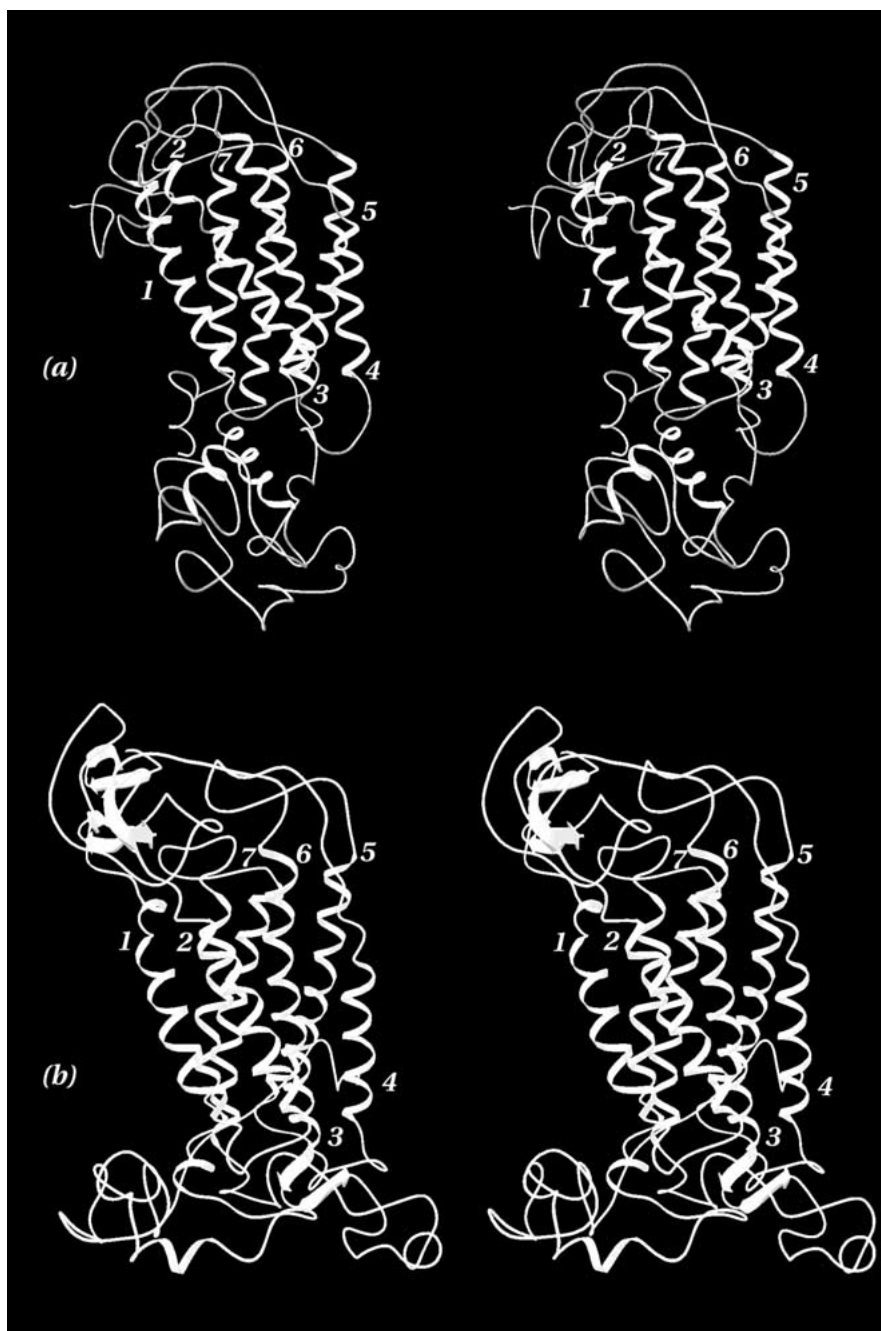


Figure 3. Overall structures of 5-HT<sub>1A</sub> (a) and 5-HT<sub>2A</sub> (b) receptor models. View along the plane of membrane, perpendicularly to the long axis of the receptor. Seven TMHs are represented as ribbons and specified by numbers. The N-terminus and extracellular loops (ECLs) are at the top of the panel, while intracellular loops (ICLs) and the C-terminus are at the bottom of the panel (below the TMHs).

residues in TMH6, serine in TMH7) were preliminary considered. Finally, two positions that gave the best ligand-receptor fit were selected for further MD simulations. In all considered positions the ligand was placed with the protonated amino group in a close vicinity (2–4 Å) to the conserved aspartic D3.32. In the ligand-5-HT<sub>1A</sub> complexes in position 1 the aromatic moiety of the ligand was close to the serine residue (S3.39) and to the highly conserved tryptophane residue (W6.50). The imide moiety of the ligand was directed towards leucine L2.55, aromatic F/W residue (3.28) (F112 in 5-HT<sub>1A</sub>, W151 in 5-HT<sub>2A</sub>, respectively), and tyrosine Y7.43. In position 2 the aromatic ligand moiety was placed in the direction of the aromatic residue (3.28), conserved phenylalanine residues: 5.47, 6.44, and 6.51. The imide moiety was oriented towards the highly conserved aspartic acid residue D2.50, and the conserved serines: S3.40 and S7.46.

Differences in affinities of the investigated compounds towards 5-HT<sub>1A/2A</sub> receptors can be explained in terms of different structures of ligand-receptor complexes. In order to explain the differences in binding affinities of buspirone analogues towards the 5-HT<sub>1A</sub> and 5-HT<sub>2A</sub> receptors, selected pairs of ligand-receptor complexes (ligand-5-HT<sub>1A/2A</sub>) were studied for each ligand. Obtained ligand-receptor complexes with the same ligand docked in two different positions were examined in order to find the most realistic position of the ligand inside the receptor. Additionally, structures of obtained ligand-receptor complexes were compared with our previous results obtained for non-methylated analogues (buspirone and kaspar) [30], in order to explain the influence of methylation of the piperazine ring on binding affinities.

#### *Interactions between ligands and 5-HT<sub>1A</sub> receptor*

After the MD simulations of the ligand-receptor complexes close atom-atom contacts between ligand and receptor amino acids can be observed. These close contacts, interpreted as main contributors to the ligand-receptor interactions, can be briefly described in the following way: in position 1; the aromatic (pyrimidinyl) moiety of (1) interacts with residues in TMHs: 2, 3, 6 and 7 (but not TMH5); the aromatic (quinoline) moiety of (2) interacts with amino acids in TMHs: 3, 5, 6 and 7 (but not TMH2); the aromatic (pyrimidinyl) moiety of (3) interacts with residues in TMHs: 3, 6 and 7 (but not TMH2 or TMH5); the piperazine ring of both (1) and (2) interacts with residues in

TMHs: 2, 3 and 7; the piperazine ring of (3) interacts with amino acids in TMHs: 1, 2, 3 and 7; the *n*-butyl moiety of (1) interacts with residues in TMHs: 1, 3 and 7, while these of (2) and (3) interact with amino acids in TMHs: 1 and 2, the *n*-butyl moiety of (3) also interacts with residues in E1; the imide moieties of (1) and (2) interact with residues in TMHs: 1, 2, 3 and 7, those of (1) also interacts with residues in E1 and E2, and the imide moiety of (3) interacts with amino acids in TMHs: 2, 3, 7 and E2.

In position 2; the aromatic (pyrimidinyl) moieties of (1) and (3) interact with residues in TMHs: 3, 5, 6, 7 and E2; the aromatic (quinoline) moiety of (2) interacts with amino acids in TMHs: 4, 5, 6 and 7 (but not TMH3 and E2); the piperazine rings of all ligands interact with residues in TMHs: 3, 6 and 7, the piperazine ring of (2) also interacts with residues in E2; the *n*-butyl moiety of (1) and (3) interacts with amino acids in TMHs: 6 and 7, while that of (2) interacts with residues in TMH3; the imide moiety of (1) and (3) interacts with amino acids in TMHs: 2, 3 and 7, while the imide moiety of (2) interacts with amino acids in TMHs: 1, 2, 7 and E2. Details are shown in Table 3.

The (2)-5-HT<sub>1A</sub> complexes are shown in Figure 4. In position 1, close atom-atom contacts between the ligand and residues in TMHs: 1, 2, 3, and 7 seem to be very important. In position 2 the most important contacts are observed for residues in TMHs: 3, 6, and 7, while contacts with residues in TMHs: 1 and 2 are rarely observed, except for the imide moiety. Compounds (1) and (3) in position 2 have very similar location and conformation at the binding site after MD. The conformation and location of compound (2) after MD simulation are different from those of (1) or (3). The binding mode of (2) after MD was very similar to the binding mode of non-methylated high affinity buspirone analogues, which were examined in our previous study [30]. This may suggest that the high affinity ligands adopt similar orientation at the binding site after MD in position 2, while the ligands with lower affinity adopt different position after MD. In position 1 each compound takes slightly different location inside the receptor and a correlation between location and affinity is not observed. This may indicate the position 2 as more realistic for docking of buspirone analogues. It also suggests that the direct contacts between ligand and receptor amino acid residues in TMHs: 3, 6, and 7 are important for high affinity binding to the 5-HT<sub>2A</sub> receptor.



**Table 3.** Ligand binding towards 5-HT<sub>1A</sub> serotonin receptor. A ligand moiety (aromatic, piperazine, butyl, imide) is considered as interacting with the residue whenever the van der Waals contacts (plus 20%) becomes smaller than a given threshold. The one letter amino acid notation, with the sequence number, are used, together with standard GPCRDB notation (in brackets)

Ligand	Aromatic moiety		Piperazine ring		<i>n</i> -butyl moiety		Imide moiety	
	Position 1	Position 2	Position 1	Position 2	Position 1	Position 2	Position 1	Position 2
(1)	T81(2.49),	I113(3.29), T188(E2),	V85(2.53), L88(2.56),	D116(3.32),	L46(1.42),	W358(6.48),	L43(1.39), L46(1.42),	V85(2.38), L88(2.4),
	V85(2.53),	I197(5.40), Y198(5.41),	V89(2.57),	V117(3.33),	D116(3.32),	F361(6.51),	M92(2.60), L99(E1),	V89(2.42), M92(2.60),
	C119(3.35),	L366(6.56),	D116(3.32),	C120(3.36), F361(6.51),	C120(3.36),	G389(7.42),	F112(3.28),	F112(3.28),
	S123(3.39),	P369(6.59), L381(7.34),	C120(3.36),	F362(6.52),	N386(7.39),	N392(7.45),	I113(3.29), A186(E2),	D116(3.32),
	W358(6.48),		G389(7.42)	A365(6.55),	G389(7.42),		G382(7.35),	N386(7.39),
	N392(7.45),			I385(7.38)	Y390(7.43)		I385(7.38)	G389(7.42)
	S393(7.46),							Y390(7.43),
	N396(7.49)							S393(7.46)
(2)	S123(3.39),	G174(4.63),	T81(2.49), L88(2.56),	I113(3.29), D116(3.32),	L46(1.42), V85(2.53),	D116(3.32),	L46(1.42), M92(2.60),	L46(1.42), V89(2.42),
	I124(3.40),	W175(4.64), T188(E2),	D116(3.32),	V117(3.33), T188(E2),	L88(2.56), V89(2.57)	V117(3.33),	F112(3.28),	M92(2.60), A186(E2),
	L127(3.43),	H193(5.36),	C119(3.35),	F362(6.52)		C119(3.35),	I113(3.29),	W358(6.48)
	F204(5.47),	G194(5.37),	C120(3.36),	A365(6.55), I385(7.38)		C120(3.36),	N386(7.39),	N386(7.39),
	L208(5.51),	T196(5.39), I197(5.40),	S393(7.46), N396(7.49)			S123(3.39)	G389(7.42),	G389(7.42),
	F354(6.44),	T200(5.43),					Y390(7.43)	Y390(7.43)
	W358(6.48),	A365(6.55),						S393(7.46)
	N396(7.49)	P369(6.59), I385(7.38)						
(3)	C119(3.35),	I113(3.29), V117(3.33),	L46(1.42), L88(2.41),	D116(3.32),	T39(1.35), L43(1.39),	W358(6.48),	V85(2.38), I113(3.29),	V85(2.38), L88(2.41),
	C120(3.36),	T188(E2), I197(5.40),	F112(3.28),	C120(3.36, F361(6.51),	V89(2.42),	F361(6.51),	C187(E2),	V89(2.42), M92(2.60),
	S123(3.39),	A365(6.55),	L115(3.31),	F362(6.52),	M92(2.60), V98(E1)	G389(7.42),	G382(7.35),	F112(3.28),
	W358(6.48),	L366(6.56, L381(7.34)	D116(3.32),	A365(6.55), I385(7.38)		Y390(7.43),	I385(7.38),	D116(3.32),
	G389(7.42),		Y390(7.43)			N392(7.45)	N386(7.39)	V117(3.33),
	N392(7.45),					S393(7.46)		N386(7.39),
	S393(7.46)							Y390(7.43),
								S393(7.46)

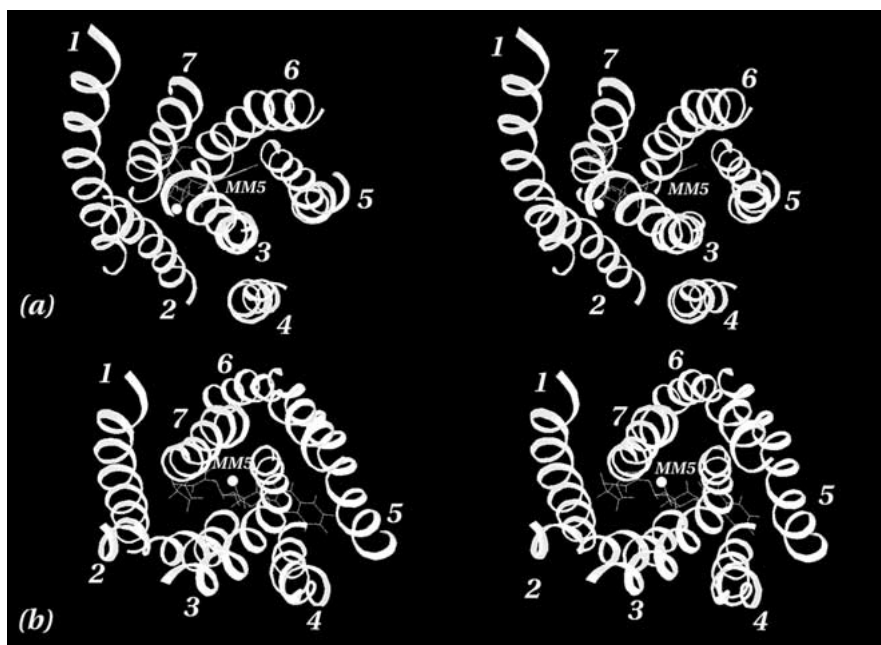


Figure 4. Stereo view of TMH bundles of average, energy-minimised (2)-5-HT<sub>1A</sub> complexes, after MD simulation. The ligand occupies position 1(a), or position 2(b). The methyl group substituted in piperazine ring is marked by the shaded circle. View from the extracellular side of the membrane, perpendicularly to the long axis of the receptor. TMHs are represented as ribbons and numbered.

Available site-directed mutagenesis data also seem to support position 2 as more realistic than position 1. Data obtained for the 5-HT<sub>1A</sub> receptor [38, 49] suggest, that amino acids important for agonist binding (such as D116(3.32) or S393(7.46)) are located in TMHs: 3, 5, 6 and 7. Also D82(2.50), highly conserved among all GPCR family, was suggested as a residue of importance for direct agonist binding [50], while Sealfon et al. [52] suggested that the role of D82 was related rather with helix-helix interactions between TMH2 and TMH7, involving D82(2.50) and N396(7.49), than with direct contact with the ligand. Also, data available for other types of GPCRs suggest that amino acids important for ligand binding are located in TMHs: 3, 6 and 7, mainly (Wieland et al., Roth et al) [63, 65]. Lappalainen et al. [66] has reported that in 5-HT<sub>2C</sub> receptor polymorphism of residues in TMH1 (S23/C23) does not cause any differences in response for serotonin. Moreover, Ling et al. [67] has found that mutants of chemokine receptors CCR5 and CXCR4 in which TMHs: 1 and 2 were deleted, were functionally correct, i.e., TMHs: 3–7 seem to be sufficient for the proper GPCR functioning. Ling et al. [67] has also suggested the possibility of existence in nature of functional GPCRs that consist of five TMHs. Taken together, available data suggest

that position 2 seems to be more realistic than position 1.

The obtained results were compared with the model of the ligand binding by GPCRs (including 5-HT<sub>1A</sub> receptor), published by Lomize et al. [41]. Although the applied methodologies were different, the results were found to be consistent. In the model proposed by Lomize et al., the ligand binding pocket of 5-HT<sub>1A</sub> consists of the residues from TMHs: 2 (V117), 3 (D116, V117 and C120), 5 (T196, I197 and T200), 6 (W358 and F362) and 7 (I385, N386, G389, T390 and S393). According to that model, the amine group of the native ligand – serotonin, should interact with the aspartic acid D116(3.32) and the aromatic ring of the ligand should be placed close to the TMHs: 4, 5, 6 and 7, interacting directly with the residues from these helices. In the present study, all these residues were found interacting directly with the examined buspirone analogues (Table 3). Also, the ligand orientation proposed by Lomize et al. [41] was very similar to the position 2, suggested in the present study for buspirone analogues. This comparison further suggests that the position 2 is a valid position for ligand docking. Thus, hereafter only position 2 is considered.

The comparison between complexes of pyrimidinyl (compounds **1** and **3**) and quinolinyl (compound **2**) derivatives shows that close atom-atom contacts are found between the aromatic moiety of the pyrimidinyl derivatives and residues in TMHs: 3, 5 and 6, but not TMH4. In the complex of 5-HT<sub>1A</sub> with the quinoline derivative (**2**) close contact was observed between the quinolinyl moiety and G174 in TMH4, but with none of the residues in TMH3 or E2. Also, in the (**2**)-5-HT<sub>1A</sub> complex very close contacts between n-butyl moiety and residues in TMH3 were observed, that were not present in the complex with neither (**1**) nor (**3**). The imide moieties of (**1**) and (**3**) interacted with residues in TMHs: 2, 3 and 7, while the imide moiety of (**2**) had close atom-atom contacts with TMHs: 1, 2, 7 and E2. Also, the location of the methyl group was different for the pyrimidinyl derivatives compared with the quinolinyl derivative. In the (**2**)-5-HT<sub>1A</sub> complex, the methyl group was oriented towards TMHs: 6 and 7 (Figure 4), while in complexes with pyrimidinyl derivatives the methyl group faced TMHs: 2 and 3.

During MD simulation of (**1**)-(b3) complexes with the 5-HT<sub>1A</sub> receptor the ligand-induced changes in the receptor structure were observed. The R.M.S. differences of TMHs between the buspirone analogues - 5-HT<sub>1A</sub> receptor complex and the free 5-HT<sub>1A</sub> receptor suggest that the main differences were found in structures of TMHs: 2, 4, 5 and 6 (Table 4), indicating, that the displacements, rotational changes and other conformational alterations of these TMHs may be important in ligand-induced receptor activation [30, 48]. In Table 4 it is shown that the compound (**2**) induced the strongest structural changes, relatively to the other compounds. This strength correlates with the binding affinity value (Table 1). These structural changes induced by (**2**) upon binding are illustrated in Figure 5. Some displacement of TMHs: 3 and 5, although relatively weaker than this induced by (**2**), was also observed for (**1**)-5-HT<sub>1A</sub> complex. The TMHs of the ligand-receptor complex moved as rigid bodies compared to the structure of the free receptor. Rigid body movements of TMHs have been observed previously in the process of rhodopsin photoactivation [45]. Helical rigid body movement has also been suggested in the activation mechanism of the muscarinic M2 receptor [46]. Results of experiments performed on the  $\beta_2$ -adrenoreceptor have also suggested that agonist induced conformational changes and displacements of TMHs: 3 and 6 are crucial for receptor activation [69]. Taken together, conformational changes and helical

Table 4. The R.M.S. differences of TMHs (backbone atoms) between the energy minimised averaged structure of 5-HT<sub>1A</sub> free receptor and the ligand-receptor complexes, docked in position 2

Helix number	Free receptor – (1)	Free receptor – (2)	Free receptor – (3)
1	0.8	1.1	0.9
2	1.5	1.9	1.6
3	1.0	1.8	1.3
4	1.2	2.0	1.4
5	1.3	1.9	1.5
6	1.6	2.4	1.3
7	0.7	1.4	0.8

rigid body motion, observed for (**2**)-5-HT<sub>1A</sub> complex, may be sign of ligand-induced receptor activation.

Compound (**2**) also induced structural changes in ICL2 and ICL3. These ligand-induced structural changes were particularly strong in the intracellular region of TMH6 and in the proximal ICL3 region (E322-R339). After MD simulation this region was found relatively closer to ICL2 than in the free receptor. It is known from site-directed mutagenesis experiments [70] that these regions of G protein-coupled receptors may be involved in direct protein-protein interactions with the G protein. Therefore, ligand-induced conformational changes in this area may reflect the activation process.

Methylated buspirone analogues influenced the hydrogen-bonding network of the 5-HT<sub>1A</sub> receptor, particularly in the region of TMHs: 2, 3 and 7. After MD simulation with ligands some hydrogen bonds existing in the free receptor were broken, while others were formed. In particular, the hydrogen bonds between N54(1.50)–D82(2.50) (ligands **1** and **3**), S123(3.39)–S393(7.46) (compound **2**, only), S123(3.39)–N396(7.49) (only ligand **2**), T81(2.49)–N396(7.49) (all ligands), and D116(3.32)–N386(7.40) (ligands **1** and **2**) were broken. Hydrogen bonds were formed between T81(2.49)–S123(3.39) (all compounds), D82(2.50)–N396(7.49) (ligands **1** and **2**), T81(2.49)–N396(7.49) (ligand **2**). These ligand-induced changes in the architecture of the hydrogen-bonding pattern can also be related to the mechanism of action of the investigated buspirone analogues. It is interesting to observe, that for buspirone and three of its non-methylated analogues [30] the hydrogen bond between N54(1.50)–D82(2.50) was conserved during all performed MD simulations.

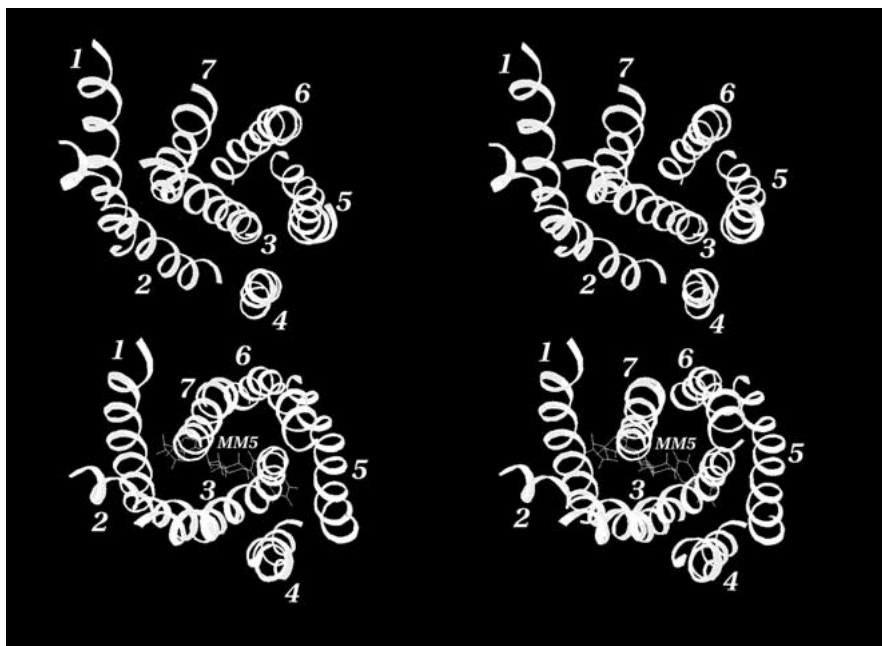


Figure 5. Structures of average, energy-minimised 5-HT<sub>1A</sub> free receptor (a) and the (2)-5-HT<sub>1A</sub> complex (b), viewed as in Figure 4. Positions of TMHs: 1 and 2 have been kept the same, to show the conformational changes and displacements of the other TMHs upon the ligand binding.

These theoretical observations correspond with experimental data. The binding affinity values of (2) and non-methylated buspirone analogues to the 5-HT<sub>1A</sub> receptor are similar, while affinity values of (1) or (3) are one order of magnitude lower (Table 1).

In order to investigate the influence of piperazine ring methylation on 5-HT<sub>1A</sub> binding the present ligand-5-HT<sub>1A</sub> receptor complexes were compared with complexes consisting of non-methylated analogues [30]. Comparison between (2)-5-HT<sub>1A</sub> and the kaspar-5-HT<sub>1A</sub> complexes showed that the methylation may slightly alter the ligand position. The difference was not very dramatic, but the structures of the ligand-receptor complexes were slightly different. However, comparison between the (1)-5-HT<sub>1A</sub> and buspirone-5-HT<sub>1A</sub> complexes showed that the methyl group in (1) alters the ligand position and thereby the geometry of the ligand-receptor complex. These structural alterations seem to be responsible for worsening of the ligand-receptor structural complementarity. It should be correlated with experimentally observed fall of the receptor affinity. The location of (3) was also altered similarly to position of (1) at the 5-HT<sub>1A</sub> receptor, compared to the buspirone-5-HT<sub>1A</sub> complex [30]. In general, a correlation between the structure of the ligand (i.e. the kind of aromatic moiety, presence/absence of methyl group in piperazine), the

structural features of the ligand-receptor complex (i.e. position of the ligand, amino acids forming close atom-atom contacts with the ligand, interhelical interactions and ligand-induced changes in hydrogen-bonding network) and the experimental affinity can be observed for the investigated buspirone analogues in the present and the previous study. Methylation of pyrimidinyl compounds attenuates the structural ligand-receptor complementarity, which in turn seems to induce lower affinity of methylated ligand towards the 5-HT<sub>1A</sub> receptor. For the (2)-5-HT<sub>1A</sub> complex, the methyl group seems to induce conformational changes that allow better accommodation of a ligand-receptor complex than of the kaspar-5-HT<sub>1A</sub> complex. The combination of a quinoline aromatic moiety and a methylated piperazine ring (as in compound 2) seems to enhance the ligand-receptor contacts in the putative binding site and induce better structural and dynamical ligand-receptor adjustment compared to the combination of a pyrimidine aromatic moiety and a methylated piperazine ring (compounds 1 and 3).

#### *Interactions between ligands and 5-HT<sub>2A</sub> receptor*

Close ligand-receptor contacts observed in complexes with 5-HT<sub>2A</sub> receptor can be described as follows: in the position 1, the aromatic (pyrimidinyl) moiety of

(1) interacted with residues in TMHs: 1, 2, 3, 5, 6 and 7; the aromatic (quinoline) moiety of (2) interacted with amino acids in TMHs: 2, 3, 5, 6 and 7; the aromatic (pyrimidinyl) moiety of (3) interacted with the residues in TMHs: 1, 2 and 7; the piperazine ring of (1) interacted with residues in TMHs: 2, 3, 6 and 7; the piperazine ring of (2) and (3) interacted with amino acids in TMHs: 2, 3, and 7; the *n*-butyl moiety of (1) interacted with residues in TMHs: 3, and 7, the *n*-butyl moiety of (2) interacted with amino acids in TMHs: 6 and 7, the *n*-butyl moiety of (3) interacted with residues in TMHs: 3, 5, 6 and 7; the imide moieties of all (1)–(3) interacted with residues in TMHs: 3, 5 and 6; additionally, the imide moiety of (1) interacts with amino acids in TMH7 and E2, and the imide moiety of (3) interacted with residues in TMH7.

In the position 2, the aromatic (pyrimidinyl) moiety of (1) interacted with amino acids in N-terminus (NT), and TMH7; the aromatic (quinoline) moiety of (2) interacted with residues in TMHs: 2, 3 and 7; the aromatic (pyrimidinyl) moiety of (3) interacted with amino acids in N-terminus (NT), and TMH2; the piperazine ring of (1) interacted with residues in TMHs: 1 and 7; the piperazine ring of (2) interacted with amino acids in TMH7; the piperazine ring of (3) interacted with residues in TMHs: 2, 3 and 7; the *n*-butyl moiety of (1) interacted with residues in TMHs: 1, 2 and 7; the *n*-butyl moiety of (2) interacted with residues in TMHs: 5 and 6; the *n*-butyl moiety of (3) interacted with amino acids in TMHs: 1 and 7; the imide moiety of (1) interacted with residues in TMHs: 2 and 3; the imide moiety of (2) interacted with amino acids in TMHs: 3, 5, 6 and 7; the imide moiety of (3) interacted with residues in TMHs: 1 and 2. More details are shown in Table 5. Structure of the (2)-5-HT<sub>2A</sub> complex is shown in Figure 6.

In the (1)-5-HT<sub>2A</sub> and (3)-5-HT<sub>2A</sub> complexes with ligands in position 1 close atom-atom contacts between the aromatic (pyrimidinyl) moiety and residues in TMHs: 1, 2, 3, 6 and 7 were observed. In the (2)-5-HT<sub>2A</sub> complex with (2) in position 1 direct interaction between the aromatic quinolinyl moiety and TMH1 were not observed. Additionally, receptor contacts with the butyl and imide moieties of the ligands involve other residues in the (2)-5-HT<sub>2A</sub> complex than in the complexes of the pyrimidinyl derivatives (1) or (3) with the 5-HT<sub>2A</sub>. However, these differences in atom-atom contacts when ligand occupies position 1 are not sufficient to explain experimentally known differences in ligand affinities towards the 5-HT<sub>2A</sub> receptor. In the complexes of the 5-HT<sub>2A</sub> receptor

with the (1) or (3) in position 2 close contacts between the ligand aromatic moiety and the residues in the N-terminus were observed. For instance, the atoms from the pyrimidinyl ring of (1) interacted with V47, N48, S49 and N54 in the N-terminus. Compound (3) interacted with S49, E50, T53 and N54 also by the pyrimidinyl ring. For the (2)-5-HT<sub>2A</sub> complex residues in the N-terminus were not involved in contacts with the ligand. Moreover, close contacts that involve amino acids in TMH1 were observed for the (1)-5-HT<sub>2A</sub> and (3)-5-HT<sub>2A</sub> complexes. In the (2)-5-HT<sub>2A</sub> complex such contacts are not observed. This result suggests that appropriate position of docking can be the position 2, as for ligand interactions with the 5-HT<sub>1A</sub> receptor. Site-directed mutagenesis data consistent with this statement were briefly described in the previous section (Roth et al. [63]). Moreover, Buck et al. [71] has reported that deletion of the N-terminal domain of 5-HT<sub>2A</sub> receptor did not affect the receptor biological activity. Also, position 2 is the one that corresponding with the position proposed by Lomize et al. for some cationic amine receptors, e.g., serotonin,  $\alpha$ -adrenergic and histamine receptors [41]. Taken together, the available results suggest that buspirone analogues should interact with amino acids that belong to TMHs: 3, 5, 6 and 7, rather than to TMH1 or the N-terminus. This statement is also consistent with the molecular modelling results for non-methylated buspirone analogues, described in our previous paper [30].

Structure-affinity relationships between were observed when comparing the structures of methylated and non-methylated analogues in complexes with the 5-HT<sub>2A</sub> receptor. As explained, such correlation was seen with the ligand in position 2, only. In position 1 we were not able to explain the influence of methylation binding affinity. Ligand induced displacements of TMH1 and the N-terminus were observed in the kaspar-5-HT<sub>2A</sub> complex but not in the (2)-5-HT<sub>2A</sub> complex, which might indicate that the methyl group of (2) prevents unfavourable conformations at the ligand. The methylation of piperazine seems to improve the appropriate structure of the ligand-receptor complex. However, comparing the (1)-5-HT<sub>2A</sub> complex (Table 5) with the buspirone-5-HT<sub>2A</sub> complex [30] indicated that the methylation of the piperazine ring seemed to cause a rather opposite effect and the affinity was lowered upon methylation. The geometries of these complexes were different. In the (1)-5-HT<sub>2A</sub> complex the displacements towards TMH1 and the N-terminus upon binding were observed. Close

Table 5. Ligand binding towards 5-HT<sub>2A</sub> serotonin receptor. Notation is described in the footnote to the Table 3

Ligand	Aromatic moiety		Piperazine ring		<i>n</i> -butyl moiety		Imide moiety	
	Position 1	Position 2	Position 1	Position 2	Position 1	Position 2	Position 1	Position 2
(1)	V84(1.42), T88(1.46), K116(2.46), S162(3.39), I163(3.40), L166(3.43), M250(5.54), V332(6.46), C336(6.49), S371(7.45)	V47(NT), D48(NT), S49(NT), N54(NT), L360(7.34), L361(7.35), F364(7.38)	L123(2.53), S159(3.36), E339(6.52), G368(7.42)	W76(1.34), S77(1.35), L80(1.38), T81(1.39), V84(1.42), D155(3.32), I367(7.41), G368(7.42)	I152(3.29), D155(3.32), V363(7.37), F364(7.38)	T81(1.39), V84(1.42), L123(2.53), S371(7.45)	V156(3.33), L228(E2), S239(5.43), F240(5.44), F243(5.47), E339(6.52), I340(6.53), I343(6.56), A359(7.33)	G124(2.54), L126(2.56), V127(2.57), V130(2.60), S131(2.61), V150(3.27), W151(3.28), L154(3.31), D155(3.32), F158(3.35)
	D120(2.50), S159(3.36), S162(3.39), I163(3.40), F243(5.47), C336(6.49), L370(7.44), S371(7.45), V374(7.48)	L123(2.53), D155(3.32), V156(3.33), F158(3.35), S159(3.36), S162(3.39), F364(7.38), I367(7.41), G368(7.42), S371(7.45)	L123(2.53), D155(3.32), S159(3.36), G368(7.42)	I152(3.29), D155(3.32), V156(3.33), A359(7.34), V363(7.37), F364(7.38)	I343(6.56), A359(7.34), V363(7.37), F364(7.38), I367(7.41), G368(7.42)	F243(5.47), C336(6.49), I340(6.53), I343(6.56)	I152(3.29), V156(3.33), L236(5.40), S239(5.43), F240(5.44), F243(5.47), W335(6.48), C336(6.49), S371(7.45), V374(7.48)	F158(3.35), S159(3.36), S162(3.39), I163(3.40), F243(5.47), W335(6.48), C336(6.49), S371(7.45), V374(7.48)
	V84(1.42), T88(1.46), D120(2.50), L123(2.53), G124(2.54), S371(7.45), V374(7.48), N375(7.49)	S49(NT), E50(NT), T53(NT), N54(NT), L126(2.50), V127(2.57), V130(2.60)	V127(2.57), D155(3.32), F364(7.38), L370(7.44)	L123(2.53), L126(2.56), W151(3.28), I152(3.29), D155(3.32), A359(7.34), V363(7.37)	D155(3.32), F243(5.47), E339(6.52), I343(6.56), V363(7.37)	V84(1.42), L360(7.35), F364(7.38), G368(7.42), Y369(7.43)	I152(3.29), V156(3.33), L236(5.40), S239(5.43), F240(5.44), F243(5.47), I343(6.56), I347(6.60), A359(7.34), V363(7.37)	T81(1.39), I85(1.43), T88(1.46), G124(2.54), M128(2.58)

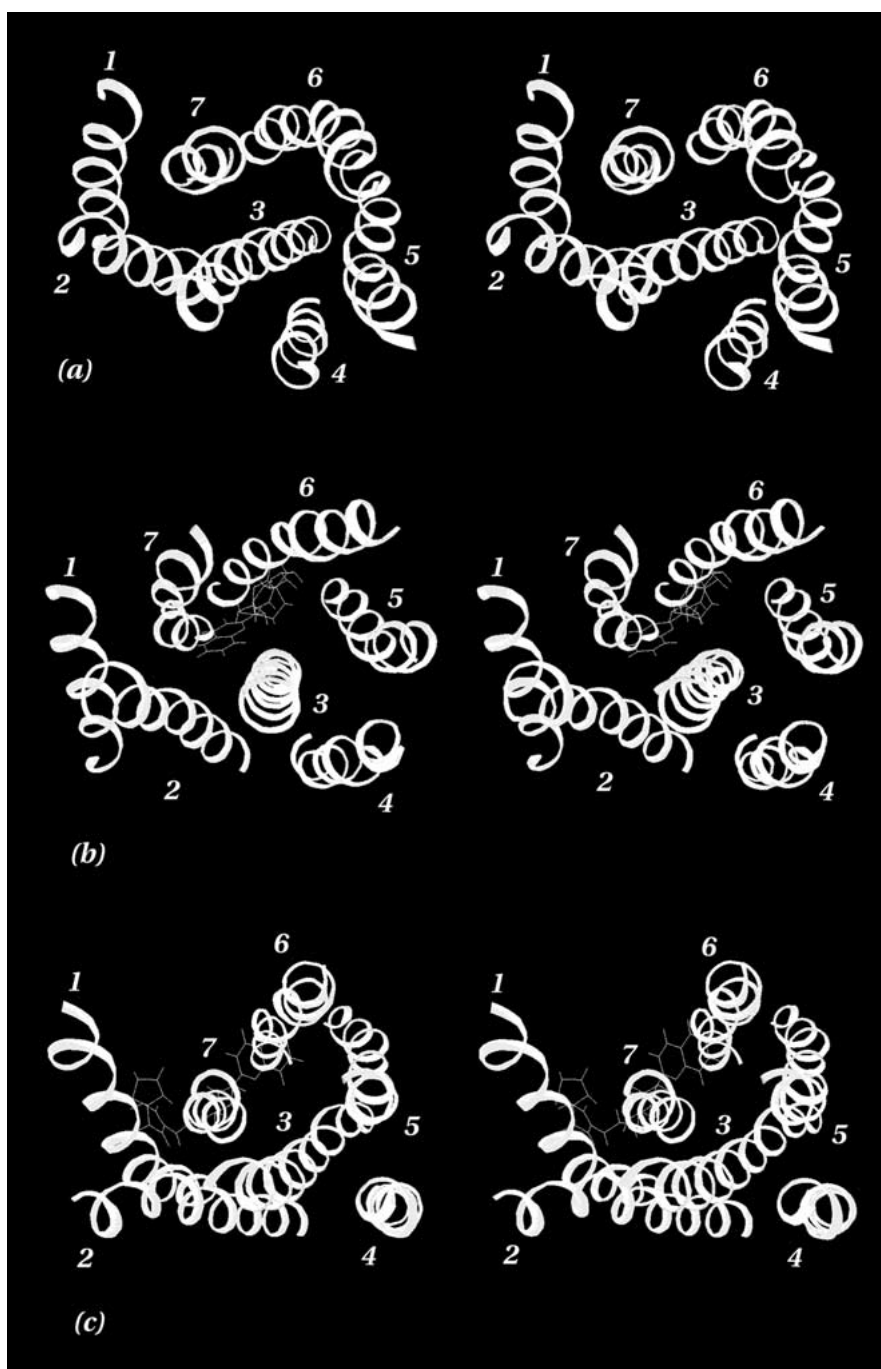


*Figure 6.* Structures of average, energy-minimised TMH bundle of 5-HT<sub>2A</sub> free receptor (a), the (2)-5-HT<sub>2A</sub> complex (b) and the Kaspar-5-HT<sub>2A</sub> complex (c), viewed as in Figures 4 and 5. Positions of TMHs: 1 and 2 have been kept the same, to show the conformational changes and displacements of the remaining part of TMH bundle upon the ligand binding. Such conformational changes were found in the (2)-5-HT<sub>2A</sub> complex, as compared to the free receptor, but the TMH bundles of the Kaspar-5-HT<sub>2A</sub> complex and the free receptor remain very similar.

contacts with residues in the N-terminus and TMH1 are characteristic for non-active analogues (Table 5). Such contacts were not observed for the buspirone-5-HT<sub>2A</sub> complex, indicating, that the 5-HT<sub>2A</sub> affinity of (**1**) should be low. Similarly to compound (**1**), the methyl group of (**3**) altered the structure of the ligand-receptor complex and the ligand position. The ligand displacement of TMH1 and the N-terminus were also observed. As for (**1**), the geometry of (**3**) inside the 5-HT<sub>2A</sub> receptor is very close to its starting structure. The conclusion that affinities of pyrimidine derivatives (i.e., **1** and **3**) should be lower than the affinity of buspirone is consistent with the experimental data [72, 73].

Replacement of the pyrimidine ring with the quinolinyl moiety while the piperazine ring is methylated seems to partly prevent the adaptation of unfavourable ligand conformations that does not produce a proper ligand-receptor binding mode. In quinolinyl derivatives the methylation of piperazine seems to induce a more proper structure of the ligand-receptor complex.

For the ligand-5-HT<sub>1A</sub> complexes in position 2 structure-affinity relationships, in respect to the structure of the aromatic moiety, methylation of the piperazine ring, structural/dynamical properties of the ligand-receptor complex and the binding affinity were observed. According to the present results methylation of compounds possessing an aromatic pyrimidinyl ring induced strong, improper constraints into the structural/dynamical complementarity between the ligand and the receptor, altering the ligand position in the central cavity of the receptor. This leads to an improper structure of the ligand-receptor complex that may lower the ligand affinity for the receptor. Methylation of a compound possessing quinolinyl moiety seems to enhance the structural/dynamical complementarity between the ligand and the receptor by altering the ligand position (Figure 6b and c). It is worth to notice, that the replacement of the pyrimidine ring by the quinolinyl moiety while piperazine is not methylated (buspirone → kaspar) caused a significant decrease (one order of magnitude, approximately) in affinity for the 5-HT<sub>2A</sub> receptor, while the same replacement in case of methylated analogues (**1** → **2**) induces better structural ligand-receptor adjustment consistent with highly increased affinity of the ligand (Table 1).

In the (**2**)-5-HT<sub>2A</sub> complex other ligand-induced changes of the receptor structure were also observed (Figure 6a and b). The R.M.S. differences of TMHs

Table 6. The RMS differences of TMHs (backbone atoms) between the energy minimised averaged structure of 5-HT<sub>2A</sub> free receptor and the ligand-receptor complexes, docked in position 2

Helix number	Free receptor – (1)	Free receptor – (2)	Free receptor – (3)
1	0.4	1.2	0.3
2	0.7	1.5	0.6
3	0.8	1.9	0.9
4	1.1	1.7	0.8
5	0.9	2.1	1.0
6	0.6	1.9	0.7
7	0.6	2.3	0.4

between the (**2**) - 5-HT<sub>1A</sub> receptor complexes and the free 5-HT<sub>2A</sub> receptor suggest that the main differences were found in structures of TMHs: 3, 5, 6 and 7 (Table 6). This was in contrast of (**1**) and (**3**) that not induced any significant structural displacement of TMHs. The obtained results indicate, as in case of the buspirone analogues-5-HT<sub>1A</sub> receptor complexes, that the displacements, rotational changes and other conformational alterations of these TMHs may be important in the receptor activation induced by ligand. The conformational changes of the receptor, induced by (**2**) during MD simulation were found to be consistent with available experimental results connecting conformational changes with the mechanism of signal transduction [46, 74].

Interactions with methylated buspirone analogues, particularly (**2**), also changed the hydrogen-bonding pattern of the receptor, compared to the free 5-HT<sub>2A</sub> receptor. However, for (**1**) and (**3**) these changes of inter-helical hydrogen-bonding network were not sufficient for inducing displacement of helices. In general, some of the hydrogen bonds present in the free receptor were broken while other hydrogen bonds were formed during MD of ligand-5-HT<sub>2A</sub> complexes. In particular, hydrogen bonds were broken between N92(1.50)–D120(2.50) (**2**), D120(2.50)–S371(7.45) (**1** and **2**), D120(2.50)–S372(7.46) (all ligands), S162(3.39)–S371(7.45) (**2**). Hydrogen bonds were created between D120(2.50)–S162(3.39) (**1** and **2**) and between D155(3.32)–S371(7.45) (**2**).

Comparison of the structures of the 5-HT<sub>1A</sub> and 5-HT<sub>2A</sub> free receptors with their ligand-receptor complexes showed that the packing of TMHs: 1, 2 and 7 relative to each other is slightly different in these two receptors. This differences influence the ligand-



receptor interactions. Y369(7.43) of the 5-HT<sub>2A</sub> receptor is faced towards the membrane, while corresponding Y390(7.43) of the 5-HT<sub>1A</sub> receptor is located in the central receptor cavity, capable to direct interactions with the buspirone analogues. Different helical packing also influences the position of the ligand inside the receptor. After MD simulation of the ligand-5-HT<sub>2A</sub> receptor complexes the aromatic moiety of the methylated ligands was oriented normal to the membrane plane, while it was oriented almost perpendicularly to the membrane plane in the complexes with the 5-HT<sub>1A</sub> receptor. In complexes with non-methylated buspirone analogues similar ligand orientations were seen both in the 5-HT<sub>1A</sub> and 5-HT<sub>2A</sub> receptors. These differences in binding site architecture of both receptors should play an important role in the ligand binding process and contribute to the affinity differences for the methylated buspirone analogues.

## Conclusions

The present results contribute to the knowledge about the structural determinants for binding selectivity of buspirone analogues for the 5-HT<sub>1A</sub> and 5-HT<sub>2A</sub> receptors. Although the obtained receptor models were constructed using the projection map of rhodopsin, and not the recent crystal structure as a guide for the TMHs packing, the huge structural similarity between the models and the crystal structure of rhodopsin has been confirmed, which proves the validity of the obtained models. The simulation length for all investigated ligand-receptor complexes was 170 ps, which is shorter than current standards for simulations of proteins. However, applied methodology allowed us to analyse the structural/dynamic changes of the human 5-HT<sub>1A</sub> and 5-HT<sub>2A</sub> receptor models upon ligand binding. These preliminary results are useful and valid as a part of study of molecular mechanism of serotonin receptor activation and the signal transduction. Results obtained on the 5-HT<sub>1A</sub> and 5-HT<sub>2A</sub> receptors, consistent with our previous results, bring important information about ligand binding modes, which will be used in the later parts of the study. Applied methodology seem to be sufficient for investigating structure-affinity relationships of the other ligands with different properties.

The results of our calculations indicated that (**2**) interacted with the 5-HT<sub>1A</sub> and 5-HT<sub>2A</sub> receptors in different manner than (**1**) or (**3**). The obtained results

also suggest that the quinolinyl derivative (**2**) fits better to both 5-HT<sub>1A</sub> and 5-HT<sub>2A</sub> putative binding sites than pyrimidinyl derivatives (**1** or **3**). The difference in binding mode of (**2**) on one side and (**1**) or (**3**) at the other side is particularly strong at the 5-HT<sub>2A</sub> receptor.

Molecular dynamics simulation suggested that position 2 is more realistic at both the 5-HT<sub>1A</sub> and 5-HT<sub>2A</sub> receptors. This result was also confirmed by the other theoretical results [41] and also by the set of site-directed mutagenesis data [63, 65–67, 71]. Amino acids that seem to be important for direct interaction with active analogues were identified. These residues could be further tested by site-directed mutagenesis experiments that may verify the present theoretical models.

It was found that the trans-membrane helical domains of the 5-HT<sub>1A</sub> and 5-HT<sub>2A</sub> receptors have slightly different topographies at the putative binding sites of the buspirone analogues. In particular, the binding site of the 5-HT<sub>1A</sub> receptor seems to be narrower than in the 5-HT<sub>2A</sub> receptor. Moreover, some differences between 5-HT<sub>1A</sub> and 5-HT<sub>2A</sub> were also found in the ligand-induced TMHs displacements and changing of hydrogen-bonding network upon ligand binding. These differences between 5-HT<sub>1A</sub> and 5-HT<sub>2A</sub> receptors may lead to their differences in ligand affinities.

The present results were found to be consistent with the experimentally detected ligand affinities for 5-HT<sub>1A</sub>/5-HT<sub>1A</sub> receptors. The present methodology may allow us to estimate the binding affinities of the other buspirone analogues and the methodology may be used to predict the influence of structural modifications on the binding affinities for 5-HT<sub>1A</sub> and 5-HT<sub>2A</sub> serotonin receptors. This may provide a rational design of compounds possessing the desired pharmacological profile and possibly better therapeutic properties.

## Acknowledgements

The present study was partially supported by the Pharmaceutical Research Institute grant. Most of the MD simulations and all *ab initio* calculations were performed using the Victorio HP V2500 supercomputer at the Informatics Department, University of Tromsø, Norway.

## References

- Westenberg, H.G., *J. Clin. Psychiatry*, 60 (1999) 4. Discussion 46.
- Cohen, M.L., Schenck, K.W., Colbert, W. and Wittenauer, L., *J. Pharmacol. Exp. Ther.*, 232 (1985) 770.
- Stockmeier, C.A., Shapiro, L.A., Dilley, G.E., Kolli, T.N., Friedman, L. and Rajkowska, G., *J. Neurosci.*, 18 (1998) 7394.
- Cusack, B., Nielson, A. and Richelson, E., *Psychopharmacology (Berl)*, 114 (1994) 559.
- Matsuoka, H., Ishii, M., Goto, A. and Sugimoto, T., *Am. J. Physiol.*, 249 (1985) Pt 1.
- Schotte, A., Janssen, P.F., Gommeren, W., Luyten, W.H., Van Gompel, P., Lessage, A.S., De Loore, K. and Leysen, J.E., *Psychopharmacology (Berl)*, 124 (1996) 57.
- Peroutka, S.J., *CNS Drugs*, 4 (1995) 18.
- Kennett, G.A., Wood, M.D., Bright, F., Cilia, J., Piper, D.C., Gager, T., Thomas, D., Baxter, G.S., Forbes, I.T., Ham, P. and Blackburn, T.P., *Br. J. Pharmacol.*, 117 (1996) 427.
- Bromidge, S.M., Dabbs, S., Davies, D.T., Duckworth, D.M., Forbes, I.T., Ham, P., Jones, G.E., King, F.D., Saunders, D.V., Starr, S., Thewlis, K.M., Wyman, P.A., Blaney, F.E., Naylor, C.B., Bailey, F., Blackburn, T.P., Holland, V., Kennett, G.A., Riley, G.J. and Wood, M.D., *J. Med. Chem.*, 7, 41 (1998) 1598.
- Bakish, D., Habin, R. and Hooper, C.L., *CNS Drugs*, 9 (1998) 271.
- Gammans, R.E., Stringfellow, J.C., Hvizdos, A.J., Seidehamel, R.J., Cohn, J.B., Wilcox, C.S., Fabre, L.F., Pecknold, J.C., Smith, W.T. and Rickels, K., *Neuropsychobiology*, 25 (1992) 193.
- Goa, K.L. and Ward A., *Drugs*, 32 (1986) 114.
- Delle Chiaie, R., Pancheri, P., Casacchia, M., Stratta, P., Kotzalidis, G.D., Zibellini, M., *J. Clin. Psychopharmacol.*, 15 (1995) 12.
- Cottraux, J., Note, I.D., Cungi, C., Legeron, P., Heim, F., Chneiweiss, L., Bernard, G. and Bouvard, M., *Br. J. Psychiatry*, 167 (1995) 635.
- Sramek, J.J., Tansman, M., Suri, A., Hornig-Rohan, M., Amsterdam, J.D., Stahl, S.M., Weisler, R.H. and Cutler, N.R., *J. Clin. Psychiatry*, 57 (1996) 287.
- Robinson, D.S., Rickels, K., Feighner, J., Fabre, L.F. Jr., Gammans, R.E., Schrotiya, R.C., Alms, D.R., Andary, J.J. and Messina, M.E., *J. Clin. Psychopharmacol.*, 10 (1990) Suppl. 67S.
- Rickels, K., Amsterdam, J.D., Clary, C., Puzzuoli, G. and Schweizer, E., *J. Clin. Psychiatry*, 52 (1991) 34.
- Aceto, M.D. and Bowman, E.R., *Arzneimittelforschung*, 43 (1993) 942.
- Giannini, A.J., Loiselle, R.H., Graham, B.H. and Folts, D.J., *J. Subst. Abuse Treat.*, 10 (1993) 523.
- Hedlund, L. and Wahlstroem, G., *Alcohol. Alcohol.*, 31 (1996) 149.
- Hedlund, L. and Wahlstroem, G., *Alcohol. Clin. Exp. Res.*, 23 (1999) 822.
- Farid, P. and Abate, M.A., *Ann. Pharmacother.*, 32 (1998) 1362.
- Realmuto, G.M., August, G.J. and Garfinkel, B.D., *J. Clin. Psychopharmacol.*, 9 (1989) 122.
- McCormick, L.H., *Arch. Farm. Med.*, 6 (1997) 368.
- Millan, M.J., Hjorth, S., Samanin, R., Schreiber, R., Jaffard, R., De Ladonchamps, B., Veiga, S., Goument, B., Peglion, J.L., Spedding, M. and Brocco, M., *J. Pharmacol. Exp. Ther.*, 282 (1997) 148.
- Matheson, G.K., Pfeifer, D.M., Weiberg, M.B. and Michel, C., *Gen. Pharmacol.*, 25 (1994) 675-83.
- Traber, J. and Glaser, T., *Trends Pharmacol. Sci.*, 8 (1987) 432.
- Balster, R.L., *J. Clin. Psychopharmacol.*, 10 (1990) 31S.
- Kleven, M.S. and Koek, W., *J. Pharmacol. Exp. Ther.*, 276 (1996) 388.
- Bronowska, A., Leś A., Chilmoneczyk Z., Filipek S., Edvardsen Ø., Østensen R., Sylte I., *Bioorg. Med. Chem.*, 9 (2001) 881.
- Chilmoneczyk, Z., Leś A., Woźniakowska, A., Cybulski, J., Koziol, A.E. and Gdaniec, M., *J. Med. Chem.*, 38 (1995) 1701.
- Ferrin, T.E., *J. Mol. Graphics*, 6 (1988) 13.
- Pearlman, D.A., Case, D.A., Caldwell, J.W., Ross, W.S., Cheatham, T.E. III, DeBolt, S., Ferguson, D.M., Seibel, G.L. and Kollman, P.A., *Comp. Phys. Commun.*, 91 (1995) 1.
- Amber 5, Case, D.A., Pearlman, D.A., Caldwell, J.W., Cheatham, T.E. III, Ross, W.S., Simmerling, C., Darden, T., Merz, K.M., Stanton, R.V., Cheng, A., Vincent, J.J., Crowley, M., Ferguson, D.M., Radmer, R., Seibel, G.L., Chandra Singh, U., Weiner, P. and Kollman, P.A., UCSF, San Francisco, 1997.
- Cornell, W.D., Cieplak, P., Bayly, C.I. and Kollman, P.A., *J. Am. Chem. Soc.*, 115 (1993) 9620.
- Gaussian 94, Revision D.1, M.J., Frisch, G.W., Trucks, H.B., Schlegel, P.M.W., Gill, B.G., Johnson, M.A., Robb, J.R., Cheeseman, T., Keith, G.A., Petersson, J.A., Montgomery, K., Raghavachari, M.A., Al-Laham, V.G., Zakrzewski, J.V., Ortiz, J.B., Foresman, J., Cioslowski, B.B., Stefanov, A., Nanayakkara, M., Challacombe, C.Y., Peng, P.Y., Ayala, W., Chen, M.W., Wong, J.L., Andres, E.S., Replogle, R., Gomperts, R.L., Martin, D.J., Fox, J.S., Binkley, D., J., Defrees, J., Baker, J.P., Stewart, M., Head-Gordon, C., Gonzalez, and J.A. Pople, Gaussian, Inc., Pittsburgh PA, 1995.
- Filipek, S., unpublished data.
- Chanda, P.A., Minchin, M.C.W., Davis, A.R., Greenberg, L., Reilly, Y., McGregor, W.H., Bhat, R., Lubeck, M.H., Mizutani, S. and Hung, P.P., *Mol. Pharmacol.*, 43 (1993) 516.
- Baldwin, J.M., Schertler, G.F.X. and Unger, V.M., *J. Mol. Biol.* 272 (1997) 144.
- Van Rhee, A.M. and Jacobson, K.A., *Drug. Dev. Res.*, 37 (1996) 1.
- Lomize, A.L., Pogozheva, I.D. and Mosberg, H.I., *J. Comp. Aid. Mol. Des.*, 13 (1999) 325.
- Sylte, I., Chilmoneczyk, Z., Dahl, S.G., Cybulski, J. and Edvardsen, Ø., *J. Pharm. Pharmacol.*, 49 (1997) 698.
- Bronowska, A., Molecular modelling of interactions between serotonin receptors and their ligands (doctoral dissertation), University of Warsaw, Warsaw, November 2000.
- Cook, E.H., Jr., Fletcher, K.E., Wainwright, M., Marks, N., Yan, S.Y. and Leventhal, B.L., *J. Neurochem.*, 63 (1994) 465.
- Farrens, D.L., Altenbach, C., Yang, K., Hubbel, W.L. and Khorana, H.G., *Science*, 274 (1996) 768.
- Liu, J., Blin, N., Conklin, B.R. and Wess, J., *J. Biol. Chem.*, 271 (1996) 6172.
- Fannelli, F., Menziani, C.M., Scheer, A., Cotecchia, S. and De Benedetti, P.G., *Methods*, 14 (1998) 302.
- Sylte, I., Bronowska, A., Dahl, S.G., *Eur. J. Pharmacol.*, 416(1-2) (2001), 33.
- Ho, B.Y., Karschin, A., Branchek, T., Davidson, N. and Lester, H.A., *FEBS Lett.*, 312 (1992) 259.
- Guan, X.-M., Peroutka, S.J. and Kobilka, B.K., *Mol. Pharmacol.*, 41 (1992) 695.
- Palczewski, K., Kumasaka, T., Hori, T., Behnke, C.A., Motoshima, H., Fox, B.A., Le Trong, I., Teller, D.C., Okada, T.,

- Stenkamp, R.E., Yamamoto, M. and Miyano, M., *Science*, 289 (2000) 739.
52. Sealfon, S.C., Chi, L., Ebersole, B.J., Rodie, V., Zhang, D., Ballesteros, J.A. and Weinstein, H., *J. Biol. Chem.*, 270 (1995) 16683.
  53. Zhou, W., Flanagan, C., Ballesteros, J.A., Konvicka, K., Davidson, J.S., Weinstein, H., Millar, R.P. and Sealfon, S.C., *Mol. Pharmacol.*, 45 (1994) 165.
  54. Gudermann, T., Nuernberg, B. and Schultz, G., *Clin. Investig.*, 73 (1995) 51.
  55. Samama, P., Cotecchia, S., Costa, T. and Lefkowitz, R.J., *J. Biol. Chem.*, 268 (1993) 4625.
  56. Lefkowitz, R.J., Cotecchia, S., Samama, P. and Costa, T., *Trends Pharmacol. Sci.*, 14 (1993) 303.
  57. Scheer, A., Fanelli, F., Costa, T., De Benedetti, P.G. and Cotecchia, S., *EMBO J.*, 15 (1996) 3566.
  58. Scheer, A., Fanelli, F., Costa, T., De Benedetti, P.G. and Cotecchia, S., *Proc. Natl. Acad. Sci. USA*, 94 (1997) 808.
  59. Strange, P.G., *Trends Pharmacol. Sci.*, 19 (1998) 85.
  60. Kristiansen, K., Kroeze, W.K., Willins, D.L., Gelber, E.I., Savage, J.E., Glennon, R.A. and Roth, B.L., *J. Pharmacol. Exp. Ther.*, 293 (2000) 735.
  61. Zhukovsky, E.A. and Oprian, D.D., *Science*, 246 (1989) 401.
  62. Zhukovsky, E.A., Robinson, P.R. and Oprian, D.D., *Biochemistry*, 27 (1992) 10400.
  63. Roth, B.L., Shokam, M., Choudhary, M.S. and Khan, N., *Mol. Pharmacol.*, 52 (1997) 259.
  64. Choudhary, M.S., Sachs, N., Uluer, A., Glennon, R.A., Westkaemper, R.B. and Roth, B.L., *Mol. Pharmacol.*, 47 (1995) 568.
  65. Wieland, K., Zuurmond, H.M., Krasel, C., Ijerman, A.P. and Lohse, M.J., *Proc. Natl. Acad. Sci. USA*, 93 (1996) 9276.
  66. Lappalainen, J., Zhang, L., Dean, M., Oz, M., Ozaki, N., Yu, D.H., Virkkunen, M., Wiegert, F., Linnoila, M. and Goldman, D., *Genomics*, 27 (1995) 274.
  67. Ling, K., Wang, P., Zhao, J., Wu, Y.L., Cheng, Z.J., Wu, G.X., Hu, W., Ma, L. and Pei, G., *Proc. Natl. Acad. Sci. USA*, 96 (1999) 7992.
  68. Chilmonczyk, Z., Cybulski, M., Iskra-Jopa, J., Chojnacka-Wójcik, E., Tatarczynska, E., Kłodzinska, A., Leś A., Bronowska, A. and Sylte, I., Interactions of 1,2,4-substituted piperazines, new serotonin receptor ligands, with 5-HT<sub>1A</sub> and 5-HT<sub>2A</sub> receptors., *Il Farmaco* (in press).
  69. Gether, U., Lin, S., Ghanouni, P., Ballesteros, J.A., Weinstein, H. and Kobilka, B.K., *EMBO J.*, 16 (1997) 6737.
  70. Eason, M.G. and Liggett, S.B., *J. Biol. Chem.*, 270 (1995) 24753.
  71. Buck, F., Meyerhof, W., Werr, H. and Richter, D., *Biochem. Biophys. Res. Commun.*, 178 (1991) 1421.
  72. Hoyer, D. and Schoeffter, P., *J. Recept. Res.*, 11 (1991) 197.
  73. Szelejewska-Woźniakowska, A., Chilmonczyk, Z., Cybulski, J. and Cybulski, M., unpublished data.
  74. Liu, J., Conklin, B.R., Blin, N., Yun, J. and Wess, J., *Proc. Natl. Acad. Sci. USA*, 92 (1995) 11642.
  75. Titeler, M., Lyon, R.A., Davis, K.H. and Glennon, R.A., *Biochem. Pharmacol.*, 36 (1987) 3265.
  76. Chilmonczyk, Z., Szelejewska-Woźniakowska, A., Cybulski, J., Cybulski, M., Koziół, A.E. and Gdaniec, M., *Arch. Pharm. Pharm. Med. Chem.*, 330 (1997) 146.